Improving the Performance of Compliant Motions by On-line Geometric Uncertainty Reduction *

Jan Rosell   **Luis Basañez**   **Raúl Suárez**

Institut d'Organització i Control de Sistemes Industrials (UPC), Diagonal 647, 08028 Barcelona, SPAIN
Phone: +34 (93) 4016653, Fax: +34 (93) 4016605
e-mails: rosell@ioc.upc.es, basanez@ioc.upc.es, suarez@ioc.upc.es

Abstract: The automatic planning of robotic assembly tasks usually gives rise to a sequence of compliant motions. These motions are executed using on-line sensory information to lessen the effect of modelling and sensing uncertainties affecting the task. This paper presents a procedure to estimate some geometric parameters in a planar assembly task in order to improve the performance of compliant motions. This procedure is part of a two-phase fine-motion planner for robotic assembly tasks in the plane, developed by the authors.

1   Introduction and overview

The automation of assembly tasks with robots requires the execution of a sequence of compliant motions when the geometric constraints of the task are used to guide the robot towards its goal. The planning of such a sequence of motions can be done following different approaches like the LMT approach [4], the two-phase approach (e.g. [10]) and the contact-space approach (e.g.[9]).

Following the two-phase approach, the authors have proposed a fine-motion planner [7][8] which:

- Generates an exact cell partition of the free and of the contact Configuration Space ($\mathcal{C}_{free}$ and $\mathcal{C}_{contact}$, respectively), and describes them by two graphs, G_{free} and $G_{contact}$, whose nodes represent configurations and whose arcs represent motions between them (either in $\mathcal{C}_{free}$ or $\mathcal{C}_{contact}$).

- Searches G_{free} to find a nominal solution path in $\mathcal{C}_{free}$.

- Models uncertainty and evaluates its effect on the nominal solution path. As a result, the arcs in $\mathcal{C}_{free}$ are classified as *non-ambiguous* when the contact situations during motion can be identified or they do not prevent the desired motion, or as *ambiguous* otherwise.

- Searches in $G_{contact}$ for alternatives in $\mathcal{C}_{contact}$ to all the ambiguous arcs in $\mathcal{C}_{free}$.

- Synthesizes the two components of the generalized compliant-motion commands, one devoted to follow the solution path previously found, and the other devoted to maintain the contact taking into account the effect of friction.

Within the scope of this planner, this paper is focused on the improvement of the execution of compliant motions through:

- on-line reduction of the geometric uncertainties (which eases the identification of the current contact situation)

- on-line estimation of the possible deviation from the nominal geometry (which allows a better performance of contact motions)

A different approach to the estimation of the geometric uncertainties couples this problem with the contact identification [1]. The point contact between two smooth surfaces is modelled by means of a virtual contact manipulator and the geometric uncertainties are incorporated into the corresponding kinematic model. Then, linear identification equations are derived for the geometric uncertainties and solved using Kalman filter techniques [3]. Different but related approaches are those that focus on parameter estimations for tracking tasks [2][5], where the geometry may be initially unknown.

The paper is structured as follows. Section 2 presents the synthesis of the compliant-motion commands. Section 3 deals with the uncertainty in the contact vertex and in the contact edge, and presents the procedures to estimate the position of the contact vertex and the position and orientation of the contact

edge. These estimations are used in Section 4 to modify the motion commands. Finally, Section 5 summarizes the conclusions of the work.

2 Compliant-motion synthesis

The generalized damping control mode is assumed. The velocity commands sent to the robot are computed from two velocity components, $\vec{v_f}$ and $\vec{v_t}$.

The compliant component, $\vec{v_f}$, has as aim to maintain a constant bounded force during motion in $\mathcal{C}_{contact}$. Given a desired reaction force $\vec{F_d}$, a force control loop with a PID controller is used to generate $\vec{v_f}$ as follows. The input to the PID controller is the force error between the desired reaction force and the actual measured reaction force. The output, multiplied by a predefined accommodation matrix, is the compliant component $\vec{v_f}$. $\vec{F_d}$ is continuously updated considering the current contact configuration and the effect of friction.

The $\vec{v_t}$ component tries to follow the nominal solution path either in $\mathcal{C}_{free}$ or $\mathcal{C}_{contact}$. Computation of $\vec{v_t}$ in $\mathcal{C}_{free}$ and in $\mathcal{C}_{contact}$ is similar, and the rest of this Section is dedicated to its determination in $\mathcal{C}_{contact}$.

Let $\mathcal{A}$ and $\mathcal{B}$ be two polygons describing a manipulated object and an static object, respectively. Let $\{W\}$ and $\{T\}$ be the reference frames attached to the workspace and to object $\mathcal{A}$, respectively. $\{T\}$ has the origin at the reference point of $\mathcal{A}$, and an orientation ϕ with respect to $\{W\}$. Each vertex of $\mathcal{A}$ is described in $\{T\}$ by a vector $\vec{h}$, with module h and orientation γ. The vertices of $\mathcal{B}$ are described in $\{W\}$ by their coordinates x and y.

Two types of basic contacts can take place: an edge of $\mathcal{A}$ against a vertex of $\mathcal{B}$ (Type-A) and a vertex of $\mathcal{A}$ against an edge of $\mathcal{B}$ (Type-B).

Let us define:

Configuration: Position and orientation of $\{T\}$ with respect to $\{W\}$.

$\mathcal{C}$-*face*: Set of contact configurations involving only one basic contact.

$\mathcal{C}$-*edge*: Set of contact configurations involving two basic contacts.

$\mathcal{C}$-*item*: Set of connected configuration of a $\mathcal{C}$-face that can be expressed as a positive linear combination of configurations of two particular $\mathcal{C}$-edges of the $\mathcal{C}$-face. The set of all $\mathcal{C}$-items is an exact cell partition of $\mathcal{C}_{contact}$ [8].

$\mathcal{C}$-*arc*: Path over a $\mathcal{C}$-item that connects two of its configurations.

$\mathcal{C}$-*path*: Sequence of $\mathcal{C}$-arcs that define the nominal solution path in $\mathcal{C}_{contact}$.

The component $\vec{v_t}$ is determined as the tangent direction to the corresponding $\mathcal{C}$-arc of the $\mathcal{C}$-path at the current contact configuration. The expressions of the $\mathcal{C}$-arcs for a given orientation are computed below from the expressions of the $\mathcal{C}$-faces and $\mathcal{C}$-edges:

$\mathcal{C}$-*face*: For a given orientation ϕ, the contact positions corresponding to the occurrence of a basic contact is expressed by a segment, $f(\phi)$, whose supporting line is:

$$x \cos \psi_W + y \sin \psi_W = d_f(\phi) \qquad (1)$$

where $d_f(\phi)$ is computed as follows. Let ψ_T and ψ_W be the orientation of the normal to the contact edge with respect to $\{T\}$ and $\{W\}$, respectively. ψ_T is a constant value for a type-A basic contact, and ψ_W for a type-B basic contact. They are related to each other by the following expression:

$$\psi_W = \psi_T + \phi + \pi \qquad (2)$$

Let d_W and d_T be the oriented distances between the straight line that supports the contact edge and the origins of $\{W\}$ and $\{T\}$, respectively. If (x_e, y_e) is a point of the contact edge, then:

$$d_W = x_e \cos \psi_W + y_e \sin \psi_W \qquad (3)$$
$$d_T = x_e \cos \psi_T + y_e \sin \psi_T \qquad (4)$$

Then, for a type-A basic contact involving the vertex with coordinates (x_v, y_v), the distance $d_f(\phi)$ is given by:

$$d_f(\phi) = x_v \cos \psi_W + y_v \sin \psi_W + d_T \qquad (5)$$

For a type-B basic contact involving the vertex with coordinates $(h_v \cos \gamma_v, h_v \sin \gamma_v)$, $d_f(\phi)$ is given by:

$$d_f(\phi) = h_v \cos(\psi_W + \pi - \gamma_v - \phi) + d_W \qquad (6)$$

$\mathcal{C}$-*edge*: For a given orientation ϕ, the contact position (x, y) corresponding to the simultaneous occurrence of two basic contacts, i and j, is obtained from the system of equations of the supporting lines of each basic contact given by equation (1) [6][8]:

$$x = \frac{d_{fi} \sin \psi_{Wj} - d_{fj} \sin \psi_{Wi}}{\sin(\psi_{Wj} - \psi_{Wi})}$$
$$y = -\frac{d_{fi} \cos \psi_{Wj} - d_{fj} \cos \psi_{Wi}}{\sin(\psi_{Wj} - \psi_{Wi})} \qquad (7)$$

$\mathcal{C}$-*arc*: Let c be a configuration, with orientation ϕ, of a $\mathcal{C}$-arc between two contact configurations n_i and n_g of a given $\mathcal{C}$-item. Let $e_1(\phi)$ and $e_2(\phi)$ be the two configurations of the $\mathcal{C}$-edges associated to the $\mathcal{C}$-item for an orientation ϕ. Then, c satisfies:

$$\overrightarrow{e_1 c} = \alpha(\phi)\, \overrightarrow{e_2 e_1} \qquad (8)$$

with

$$\alpha(\phi) = \alpha_i + (\alpha_g - \alpha_i)\frac{\phi - \phi_i}{\phi_g - \phi_i} \qquad (9)$$

where ϕ_g and ϕ_i are the orientations of n_g and n_i, respectively, and α_i and α_g are determined from (8) for $c = n_g$, $\phi = \phi_g$ and $c = n_i$, $\phi = \phi_i$, respectively.

3 Uncertainty analysis

This Section presents how the effect of the uncertainty is modelled on the contact edges and vertices, and how, taking into account configuration information, this uncertainty can be reduced and the actual location of the vertices and edges be estimated.

The considered modelling and sensing uncertainties include: a) manufacturing tolerances, b) imprecision in the positioning of the static objects, c) imprecision in the positioning of the manipulated object in the robot gripper, and d) imprecision in the position and orientation of the robot.

It is assumed that the objects are positioned in such a way that the actual vertices lie anywhere inside circles centered on the nominal position of the nominal vertices. Let ϵ_v and ϵ_e be the radius of these circles for the contact vertex and vertices of the contact edge, respectively.

The uncertainty on the position of the contact vertex is given by a circle, $\mathbf{V}_v$, of radius ϵ_v centered on the nominal position of the vertex.

The uncertainty on the position of e is given by the uncertainty region, $\mathbf{E}(\beta)$, that contains all the possible realizations of e for a given deviation β in its orientation [8] (Figure 1). $\mathbf{E}(\beta)$ is computed assuming that the actual vertices of the contact edge lie inside circles, $\mathbf{V}_{v_A}$ and $\mathbf{V}_{v_B}$, of radius ϵ_e centered at their nominal position, and that the orientation of e has a given deviation β.

Let R_β be the range of possible values of β, and l_0 the nominal length of e, and assume that due to the
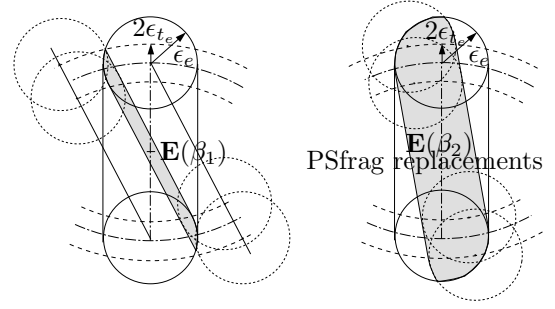

Figure 1: *Region* $\mathbf{E}(\beta)$ *of possible positions of the contact edge for two deviations in its orientation.*

manufacturing tolerances the vertices of e lie inside circles of radius ϵ_{t_e}. Then the maximum range of R_β is [8]:

$$R_\beta = [-\beta_{max}, \beta_{max}] \qquad (10)$$

with

$$\beta_{max} = \begin{cases} \arcsin(\frac{\epsilon_e}{l_0/2}) & \text{if } (l_0 - \sqrt{l_0^2 - 4\epsilon_e^2})/2 \le \epsilon_{t_e} \le \epsilon_e \\ 2\arcsin(\sqrt{\frac{\epsilon_e^2 - \epsilon_{t_e}^2}{l_0(l_0 - 2\epsilon_{t_e})}}) & \text{otherwise} \end{cases} \qquad (11)$$

3.1 Uncertainty in the contact vertex

Uncertainty reduction

Given a basic contact i that occurs at the current observed configuration $c_o = (x_o, y_o, \phi_o)$, then the region where the actual contact vertex lies can be reduced from $\mathbf{V}_v$ to:

$$\mathbf{V}_v \cap \mathbf{E}(0) \qquad (12)$$

represented by a dark shaded region in Figure 2a.

Estimation of the position of the contact vertex

The position of the contact vertex is estimated as the center of the maximum circumference inscribed into the region $\mathbf{V}_v \cap \mathbf{E}(0)$. It is computed as follows.

Let us define the following distances in the normal direction to the contact edge (Figure 2):

- Distance d_1:

$$d_1 = \min\{(x_v - x_e)\cos\psi + (y_v - y_e)\sin\psi - \epsilon_e, -\epsilon_v\} \qquad (13)$$

  It is the signed distance from the nominal position of the contact vertex to the line containing the external border of $\mathbf{E}(0)$, bounded by $-\epsilon_v$.
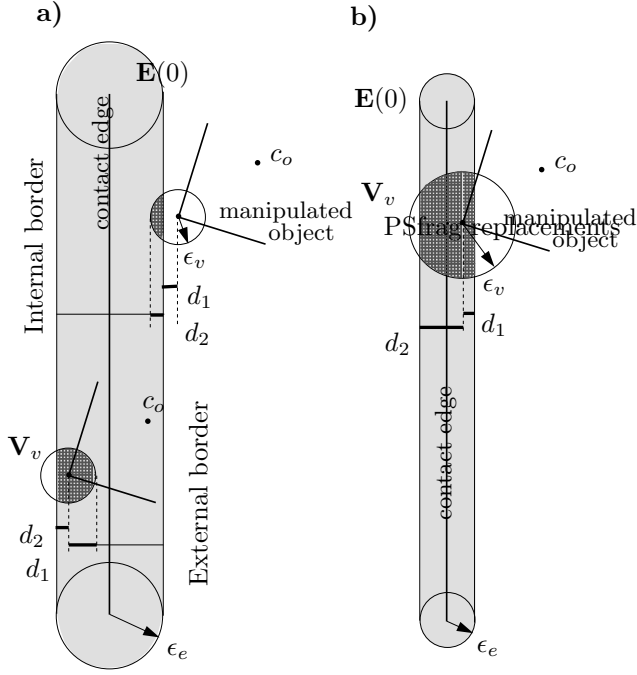
Figure 2: *Distances d_1 and d_2 in a type-B basic contact where a) $\epsilon_e > \epsilon_v$ b) $\epsilon_e < \epsilon_v$.*

- Distance d_2:

$$d_2 = \max\{(x_v - x_e)\cos\psi + (y_v - y_e)\sin\psi - \epsilon_e, \epsilon_v\} \quad (14)$$

  It is the signed distance from the nominal position of the contact vertex to the line containing the internal border of $\mathbf{E}(0)$, bounded by ϵ_v.

Then, the center of the region $\mathbf{V}_v \cap \mathbf{E}(0)$ is located at a distance $d_3 = \frac{d_1 + d_2}{2}$ from the nominal vertex position. Therefore, the estimation of the position of the contact vertex with nominal coordinates (x_v, y_v) is:

$$V_e = (x_{ve}, y_{ve}) = (x_v + d_3\cos\psi, y_v + d_3\sin\psi) \quad (15)$$

For type-B basic contacts the estimated vertex will be expressed as (Figures 3):

$$
\begin{aligned}
h_{v_e} &= \sqrt{x_{v_e}^2 + y_{v_e}^2} \\
\gamma_{v_e} &= \arctan(x_{v_e}/y_{v_e}) \quad (16)
\end{aligned}
$$

3.2 Uncertainty in the contact edge

Uncertainty reduction

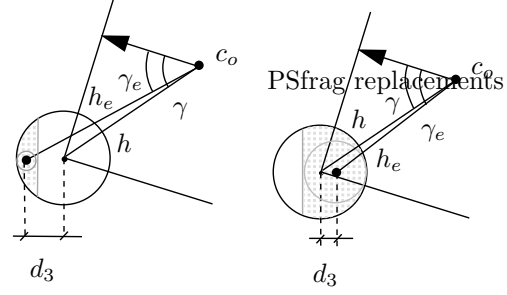Let us consider the basic contact situation of Figure 4a that occurs at the current observed configuration

Figure 3: *Estimation of the position (h_e and γ_e) of the contact edge.*

$c_o = (x_o, y_o, \phi_o)$. The uncertainty in the orientation of e is initially given by $R_\beta = [-\beta_{max}, \beta_{max}]$ (Figure 4b). Since the observed configuration is a contact configuration, then e intersects $\mathbf{V}_v$. This reduces the range R_β, as shown in Figure 4c.

The limits of R_β are determined from the three constraints that the contact edge e must satisfy:

$$
\begin{aligned}
e \cap \mathbf{V}_{v_A} &\neq \emptyset \quad (17) \\
e \cap \mathbf{V}_{v_B} &\neq \emptyset \quad (18) \\
e \cap \mathbf{V}_v &\neq \emptyset \quad (19)
\end{aligned}
$$

Then:

- From (17) and (18), $\beta \in [-\beta_{max}, \beta_{max}]$.
- From (17) and (19), $\beta \in [\beta_{min}^A, \beta_{max}^A]$.
- From (18) and (19), $\beta \in [\beta_{min}^B, \beta_{max}^B]$.

The range $[\beta_{min}^A, \beta_{max}^A]$ is the range of orientations intersecting both $\mathbf{V}_v$ and $\mathbf{V}_{v_A}$, and $[\beta_{min}^B, \beta_{max}^B]$ is the range of orientations intersecting both $\mathbf{V}_v$ and $\mathbf{V}_{v_B}$. These ranges, computed below, depend on the current configuration and are updated for each new observed contact configuration. Then, the range R_β after the first observation is:

$$
\begin{aligned}
R_\beta &= [-\beta_m, \beta_M] \quad (20) \\
\beta_m &= \max(-\beta_{max}, \beta_{min}^A, \beta_{min}^B) \quad (21) \\
\beta_M &= \min(\beta_{max}, \beta_{max}^A, \beta_{max}^B) \quad (22)
\end{aligned}
$$

And for each new observed contact configuration, R_β is updated with the new values of β_m and β_M:

$$
\begin{aligned}
\beta_m &= \max(\beta_m, \beta_{min}^A, \beta_{min}^B) \\
\beta_M &= \min(\beta_M, \beta_{max}^A, \beta_{max}^B) \quad (23)
\end{aligned}
$$

In order to obtain β_{min}^A, β_{max}^A, β_{min}^B and β_{max}^B, let us define the following nomenclature associated to a given basic contact (Figure 5):
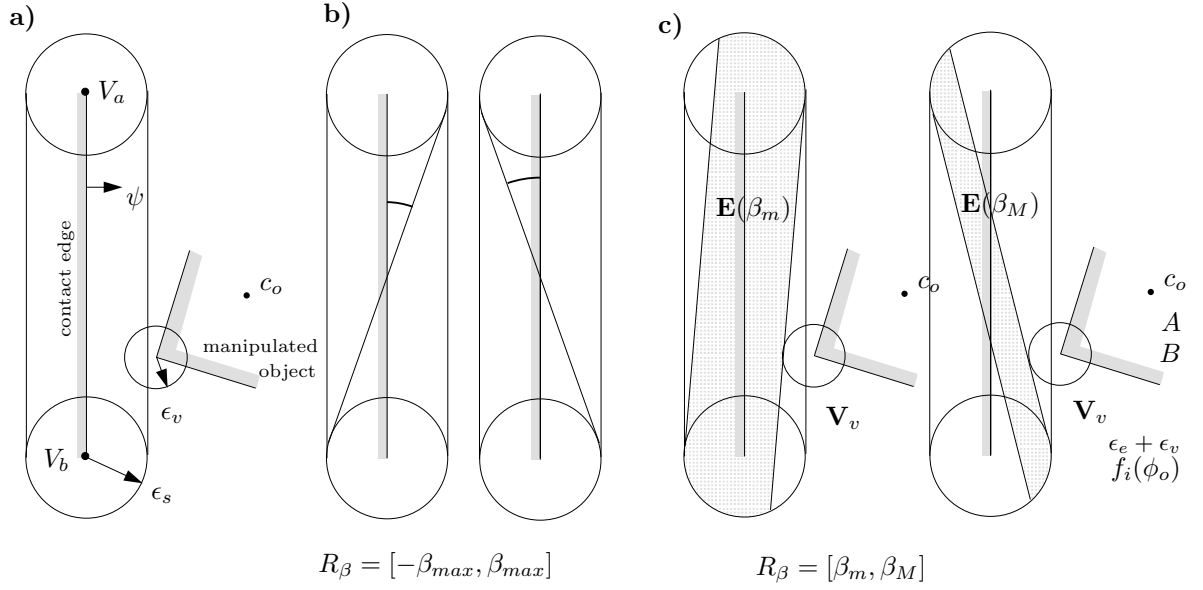
Figure 4: *a) Topological elements involved in a type-B basic contact, b) minimum and maximum deviation of the orientation of the contact edge due to uncertainty, c) minimum and maximum deviation of the orientation of the contact edge due to uncertainty, for a given observed contact configuration c_o.*

V_a and V_b: vertices of the contact edge such that V_a is first encountered when the border of the object is followed clockwise.

V: contact vertex

$\vec{e}$: vector with origin at V_a and extreme at V_b.

$\vec{r}$: vector with origin at V_a and extreme at V.

δ_A, ξ_A: the following angles:

$$\delta_A = \arcsin\left(\frac{\vec{e} \times \vec{r}}{|\vec{e}||\vec{r}|}\right) \qquad (24)$$

$$\xi_A = \arcsin\left(\frac{\epsilon_e + \epsilon_v}{|\vec{r}|}\right) \qquad (25)$$

Then:

$$\begin{aligned} \beta_{min}^A &= \delta_A - \xi_A \\ \beta_{max}^A &= \delta_A + \xi_A \end{aligned} \qquad (26)$$

In an analogous way:

$$\begin{aligned} \beta_{min}^B &= \delta_B - \xi_B \\ \beta_{max}^B &= \delta_B + \xi_B \end{aligned} \qquad (27)$$

Estimation of the orientation of the contact edge

The new estimated value β_e of β is choosen as the middle value of the range R_β of possible deviations:

$$\beta_e = \frac{\beta_M + \beta_m}{2} \qquad (28)$$

The initial estimated value is $\beta_e = 0$ corresponding to the edge nominal orientation, since initially $R_\beta = [-\beta_{max}, \beta_{max}]$.

Estimation of the position of the contact edge

Given the estimation of the position of the contact vertex, (v_{x_e}, v_{y_e}), and of the deviation in the orientation of the contact edge, β_e, the estimation of the distances d_T and d_W, which determine the position of the contact edge, are given by the values for which the estimated contact edge contains the estimated contact vertex:

$$d_{W_e}(\phi_o) = x_{v_e} \cos(\psi_W + \beta_e) + y_{v_e} \sin(\psi_W + \beta_e) \qquad (29)$$

$$d_{T_e}(\phi_o) = x_{v_e} \cos(\psi_T + \beta_e) + y_{v_e} \sin(\psi_T + \beta_e) \qquad (30)$$

4 Modification of the $\mathcal{C}$-arcs

The $\mathcal{C}$-arcs determined off-line from the nominal geometry (equations (8) and (9)), are modified on-line
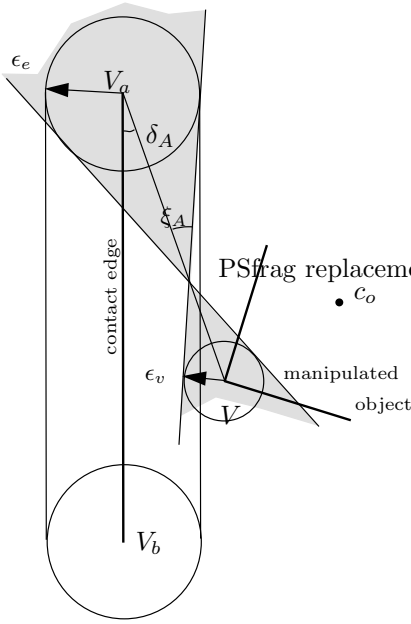
Figure 5: *Computation of the range of orientations of the lines that intersect the circumference where the contact vertex lies and the circumferences where V_a lie.*

by changing, in the expression of the $\mathcal{C}$-edges described by equation (7), the nominal values describing the position of the contact vertex and the position and orientation of the contact edge by the corresponding estimated values computed as it is described in the previous sections.

Let ψ_{W_e} and $d_{f_e}(\phi_o)$ be the estimations of ψ_W and $d_f(\phi_o)$, respectively:

$$\psi_{W_e} = \psi_W + \beta_e \qquad (31)$$

For a type-A basic contact:

$$d_{f_e}(\phi_o) = x_{v_e} \cos \psi_{W_e} + y_{v_e} \sin \psi_{W_e} + d_{T_e} \qquad (32)$$

For a type-B basic contact:

$$d_{f_e}(\phi_o) = h_{v_e} \cos(\psi_{W_e} + \pi - \gamma_{v_e} - \phi_o) + d_{W_e} \qquad (33)$$

Then, the modified expressions of the $\mathcal{C}$-edges are the following:

$$
\begin{aligned}
x &= \frac{d_{f_e i} \sin \psi_{W_e j} - d_{f_e j} \sin \psi_{W_e i}}{\sin(\psi_{W_e j} - \psi_{W_e i})} \\
y &= -\frac{d_{f_e i} \cos \psi_{W_e j} - d_{f_e j} \cos \psi_{W_e i}}{\sin(\psi_{W_e j} - \psi_{W_e i})}
\end{aligned} \qquad (34)
$$

From these $\mathcal{C}$-edges the $\mathcal{C}$-arcs are determined by expressions (8) and (9).

5 Conclusions

The paper has proposed a procedure for the on-line reduction the geometric uncertainty in order to improve the performance of compliant motions. This procedure is part of a two-phase fine-motion planer for assembly tasks in the plane. Compliant-motion commands, synthesized off-line from the nominal geometry, are recomputed on-line by estimating the possible deviations of the geometric parameters of the contact situations. Configuration sensory information is used for the estimation of the position and orientation of the contact edge and the position of the contact vertex. The computations are simple enough to be performed on-line.

References

[1] Bruyninckx H., Demey S. Dutré S., and J. De Schutter "Kinematic Models for Model-Based Compliant Motion in the Presence of Uncertainty" *Intl. J. Robotics Research*, Vol. 14, No. 5, 1995, pp. 465-482.

[2] De Schutter J. and H. Van Brussel "Compliant Robot Motion I. A formalism for specifying compliant motion tasks." *Intl. J. Robotics Research*, Vol 7, No. 4, 1988, pp. 3-17.

[3] Dutré S., Bruyninckx H., Demey S. and J. De Schutter "Solving Contact and Grasp Uncertainties" *Proc. of the 1997 IEEE IROS*, pp. 114-119.

[4] T. Lozano-Perez, M.T. Mason and R.H. Taylor, "Automatic Synthesis of Fine-Motion Strategies" *The International Journal of Robotics Research*, Vol.3, No.1, pp.3-24, 1984.

[5] Natale C., Siciliano B. and L. Villani "Control of Moment and Orientation for a Robot Manipulator in Contact with a Compliant Environment" *Proc. of the 1998 IEEE ICRA*, pp. 1755-1760.

[6] Rosell J., Basañez L. and R. Suárez, "Embedding Rotations in Translational Configuration Space" *Proc. of the 1997 IEEE ICRA*, pp. 2825-2830.

[7] Rosell J., Basañez L. and R. Suárez, "Compliant-Motion Planning and Execution for Robotic Assembly" *Proc. of the 1999 IEEE ICRA*.

[8] Rosell J. "Fine-motion planning for robotic assembly under modelling and sensing uncertainties" Ph.D. Thesis, Polythecnical University of Catalonia, 1998. http://www.ioc.upc.es/˜rosell/tesi.html

[9] Suárez R., Basañez L. and Rosell J. "Using Configuration and Force Sensing in Assembly Task Planning and Execution" *Proc. of the 1995 IEEE Int. Symposium on Assembly Task Planning*, pp.273-279.

[10] J. Xiao and R. Volz, "On Replanning for Assembly Tasks Using Robots in the Presence of Uncertainties", *Proc. of the 1989 IEEE ICRA*, pp. 638-645.